Aerosol and Air Quality Research, 15: 648–656, 2015

ISSN: 1680-8584 print / 2071-1409 online
doi: 10.4209/aaqr.2014.04.0081

Modeling Penetration through Fibrous Filter during Dynamic Filtration

Bichao Bao[1], Weilang He[1], Huan Zhao[1], Bin Xu[2], Zhongping Lin[1*]

[1] *School of Mechanical Engineering, Tongji University, 1239 Siping Road, Shanghai 200092, China*
[2] *Department of Environmental Engineering, Tongji University, 1239 Siping Road, Shanghai 200092, China*

ABSTRACT

A model to quantitatively describe penetration change during filter clogging through a fiber filter is proposed. This model is developed using two different analytical methods and indicates that filter penetration is a function of the coefficient K and deposited dust mass in the filter. This is verified through a number of laboratory filter experiments. The coefficient K is obtained using regression analysis via the results of the experiments with different dust loading parameters. K is expressed as a function of aerosol particle diameter, efficiency, and filter material. A larger value of K illustrates a higher increasing rate of efficiency during clogging. A larger value of K also correlates with a smaller aerosol particle size and a higher penetration filter.

Keywords: Penetration model; Dynamic filtration; Fibrous filter.

INTRODUCTION

As a simple and effective way of particle removal from gas streams, fibrous filters are widely used in many industries, such as pharmaceutical, biotechnology, microelectronics and semiconductor manufacturing. Penetration and pressure drop are the most important aspects of performance of fiber filters. For clean fibrous filters, a thorough study is essential. However, only limited studies have been devoted to the penetration of a dust-loaded filter.

Watson (1946) described the general process of particles accumulation on a glass fiber where they build up in chains. The chain-like structure was examined using an electron microscope. It was observed that the ‘new fibers’ composed of the collected particles themselves, act as very efficient and perhaps more efficient collectors than the original fibers. Wright *et al.* (1957) also photographed aerosol particles that were deposited on individual glass fiber, and indicated that the nature of the aerosol and the deposition velocity had significant influence on the character of the deposit. Two liquid aerosols (with diameter of 0.3 and 1.4 microns) and one solid aerosol (with diameter of 1.2 micron) were used in the experiments. It was found that the density of compaction of the aerosol deposit was the main factor in determining the effect of dust loading on the pressure drop and collection efficiency.

In addition to observing the dust-loaded fiber, researchers also made efforts to analyze the effect of dust accumulation on filtration. Payatakes and Tien (1976) proposed a preliminary theoretical model of the formation and growth of particle dendrites-like on a single cylindrical collector during filtration. Payatakes (1977) further developed a revised and generalized version of that model. The major revisions were as following: 1) allowance was made for collisions with a particle in a given dendrite layer that lend to retention in the same layer; 2) radial as well as angular contributions to deposition were considered; and 3) the dendrite layer adjacent to the collector was allowed to contain more than one particle. That model was validated by Bhutra and Payatakes (1979). A series of elaborate designed experiments were carried out with the conditions of dominant inertial impaction and interception using monodisperse aerosol particles. The growth of several individual dendrites was followed and observed, by a photographic technique, as a function of angular coordinates and time. The theoretical rates of dendrite growth were found to be in good agreement with the experimental results. Payatakes and coworkers as well as other researchers (Payatakes and Gradoń, 1980a, b; Kanaoka *et al.*, 1980) subsequently extended this concept.

When the quantity of captured dust increases, interactions of the particles are enhanced. Then, the separation of dust can no longer be described by the single fiber-particle system alone. From the formation of dendrite onwards, the separation is almost exclusively confined to the surface of the filter medium within the newly-formed filter cake. Thus, the dust loading process for fibrous filters generally reaches the dust cake filtration region, in which particle layers are formed on the surface of the filter media. Thomas *et al.* (2001) described

[*] Corresponding author.
Tel./Fax: 86-21-65984228
E-mail address: zplin99@tongji.edu.cn

the effect of deposited particles as two stages. During the first stage, with a small increase of pressure drop, the filter efficiency grew dramatically until reaching the loading point of cake formation. However, during the second stage, the rate of efficiency increase was slow. It was quite difficult to estimate the change of efficiency due to a lack of sensitivity of the measurement. Schmidt and Löffler (1990, 1991) developed a method to freeze the dust cake structure of subsequent microscopic examination. Schmidt (1995, 1997) observed that the porosity of dust cake layer decreased with increasing pressure drop and therefore proposed a simulation program based on a simple model, by which local transient porosities inside the dust cake and the pressure drop as a function of time can be calculated. Endo *et al.* (1998) presented a new analytical equation of dust cake including the effects of polydispersity and shape-factor of the particles, which were significant effect on filter loading. Silva *et al.* (1999) proposed that with an increase in the superficial velocity of filtration, cake porosity decreased and cake specific resistance increased.

This study focused on the quantitative change of penetration of filters caused by deposited particles. Some penetration equations regarding filter clogging have been developed by researchers. By using the expression for the local fiber efficiency, Billings (1966) developed following equation to describe the change in filter penetration during clogging:

$$P_A = P_0 \exp(-SA) \tag{1}$$

where P_0 is the initial penetration, A is the number of particles deposited per cm^2 of filter face area, the average of coefficient S is 1.88×10^{-9} cm^2/p, which is related to the geometry of the deposit structures and its capture efficiency rather than the filter structure. If air velocity is constant, A is evaluated by:

$$A = U_0 N_0 \Delta t \bar{E} \tag{2}$$

where $\bar{E}$ is the average filter efficiency during the time interval Δt, U_0 is air velocity, N_0 is particle concentration. The coefficient S was obtained by testing 12 filters lapped from 10-micron fiber with 1.305-microm polystyrene particles, which ranged from 0.6×10^{-9} cm^2/p to 6.9×10^{-9} cm^2/p. Since S is a variable with different situations, the application of Eq. (1) is limited. Davies (1970) derived an equation based on some empirical correlations from his early observations:

$$P = P_0 \exp\{-[\exp(\beta t/2) - 1] \ln\gamma\} \tag{3}$$

$$\beta = \frac{1}{\Delta p}\frac{d(\Delta p)}{dt} \tag{4}$$

$$\gamma = P_0^{-1} \tag{5}$$

where t is time, P_0 is the initial penetration, Δp is the pressure drop during clogging.

Hinds (1990) proposed the filter penetration P is function of single fiber collection efficiency η and can be calculated by the following equation:

$$P = \exp\left[-\frac{4\alpha\eta Z}{d_F \pi}\right] \tag{6}$$

where α is the packing density defined as the ratio of the volume of fiber and the total filter volume, Z is the total filter thickness, d_F is the diameter of fiber. Some researchers have developed their contribution to the study of single fiber efficiency η during dynamic flirtation. Billings (1966) proposed that local collection efficiency of the fiber and the deposit can be represented in the form of an expansion as:

$$\eta_Z = \eta_0 + SY \tag{7}$$

where Y is the number of particles deposited per cm^2 of fiber cross-section normal to flow, S is found to be 1.36×10^{-9} cm^2/p. Barot *et al.* (1980) later corroborated the Billings' findings. Kanaoka *et al.* (1980) simulated the growth of particle dendrites on a fiber and developed formulas to predict the dust-loaded fiber efficiency η_m:

$$\frac{\eta_m}{\eta_0} = 1 + \lambda m \tag{8}$$

where η_0 is the efficiency of the bare fiber, λ is an empirical parameter, and m is the accumulated mass per volume filter. λ was found to depend on η_0 with a roughly inverse relationship to the efficiency η_0. Kasper *et al.* (2009) developed Eq. (8):

$$\frac{\eta_m}{\eta_0} = 1 + bm^c \tag{9}$$

where η_m, η_0, m are the same definition as Eq. (8), b and c are empirical fit coefficients. Particle Stokes number St, particle interception parameter R and fiber Reynolds number Re_F following are their conventional definitions:

$$St = \frac{\rho_P d_P^2 v}{18\mu d_F} \tag{10}$$

$$R = \frac{d_P}{d_F} \tag{11}$$

$$Re_F = \frac{v d_F}{\upsilon} \tag{12}$$

where the subscripts F and P denote the particle and fiber, respectively.

For a completely isolated fiber within their experimental condition range of $0.3 \le St \le 10$, $0.3 \le Re_F \le 10$ and $0.3 \le v \le 10$, b and c were given by the following fit functions:

$$b = 0.27\left[\frac{St}{R} - 13\right]^2 + 5 \tag{13}$$

$$c = \exp\{-1.41Re_F - 0.84\} + 0.53 \tag{14}$$

For a fiber within an array, c = 0.75 and

$$b = 0.0053\left[\frac{St}{R} - 19.8\right]^2 + 0.72 \tag{15}$$

For the last few years, researchers e.g., Dunnett and Clement (2006), Hosseini *et al.* (2012), Wang *et al.* (2012) have worked on the efficiency change of single dust-loaded fibers.

The previous work has established some theoretical and empirical models to evaluate the penetration change of filter during clogging. However, the complicated equation and insufficient accurate coefficient limit their applications. The aim of this study is to develop a practical model to quantitatively evaluate the efficiency change during the filter clogging. This model is developed using two different analytical methods and validated by experiments with different filter loading tests.

PENETRATION MODELING DURING DYNAMIC FILTRATION

There are three existing hypotheses describing the mechanism of dust deposit in the filter: (i) ignoring the specific deposit structure and, assuming captured particles fill the filter, the fiber filter material becomes more compact; (ii) assuming the deposited particles form new "fiber" on the original fiber; (iii) during the clogging process, the increasing diameter of the fiber impacts the resistance and efficiency of the filter. Hypothesis (i) and (ii) are adopted respectively in this paper to develop the model.

Deduced from First Hypothesis

Firstly, hypothesis (i) that captured particles make the filter material become more compact is used to evaluate the penetration during dynamic filtration. By logarithm on both sides of Eq. (6), it can be obtained:

$$\ln P_M = -\frac{4\alpha_M \eta Z}{d_F \pi} \tag{16}$$

where P_M is penetration of dust-loaded filter.

The packing density α_M during filtration is given as:

$$\alpha_M = \alpha_0 + \frac{M}{\rho_P BZ} \tag{17}$$

where α_0 is initial packing density, M is mass of collected particle, ρ_P is particle density, B is area of filter. Combining Eq. (16) and Eq. (17):

$$\ln P_M = -\frac{4\left(\alpha_0 + \frac{M}{\rho_P BZ}\right)\eta Z}{d_F \pi} \tag{18}$$

Initial penetration P_0:

$$\ln P_0 = -\frac{4\alpha_0 \eta Z}{d_F \pi} \tag{19}$$

Therefore, P_M is a function of P_0 defined as:

$$\ln P_M = \left(1 + \frac{M}{\alpha_0 \rho_P BZ}\right) \ln P_0 \tag{20}$$

$$\ln P_M = (1 + DM) \ln P_0 \tag{21}$$

By defining $1/\alpha_0\rho_P$ as coefficient F, and m as the accumulated mass per volume filter:

$$\ln P_m = (1 + Fm) \ln P_0 \tag{22}$$

Deduced from Second Hypothesis

Secondly, the whole fibrous filter material can be regarded as a single long fiber. Accordingly, capturing particles in filter actually can be considered as capture by the single fiber. Based on this hypothesis, Kanaoka (1990) calculated the single fiber collection efficiency by making use of the filter filtration efficiency. Eq. (6) is expressed as follows:

$$\ln P = -\frac{4\alpha \eta d_F Z}{d_F^2 \pi} = \frac{L\eta d_F}{B} \tag{23}$$

where L is the length of the single long fiber.

From Eq. (23), it can be found that the filter penetration is related to total fiber length, filter area, fiber diameter and single fiber collection efficiency. Thus, the penetration during dynamic filtration is a function of dust-loaded fiber efficiency, combining Eq. (8) and Eq. (23):

$$\ln P_m = \frac{L\eta_0(1 + \lambda m)\, d_F}{B} \tag{24}$$

$$\ln P_m = (1 + \lambda m) \ln P_0 \tag{25}$$

Replacing m with M, M is the accumulated mass in whole filter:

$$\ln P_M = (1 + KM) \ln P_0 \tag{26}$$

$$K = \lambda / BZ \tag{27}$$

Comparison of the Deduced Results

It can be found that the two formulas deduced from different methods are consistent by Eq. (21) and Eq. (26) or Eq. (22) and Eq. (25). It is shown that penetration of a clogging filter is a function of initial filter penetration, mass accumulated in the filter, and a coefficient. The coefficient can be obtained by experimental data.

A number of laboratory experiments using different filter-loading tests were carried out to validate the deduced model and obtain the coefficient. Experimental data analysis in section 3, Eq. (26) can be expressed as:

$$-\ln P_M = -(1 + KM)\ln P_0 = -\ln P_0 - (K\ln P_0)M \quad (28)$$

EXPERIMENTAL VALIDATION OF THE DEDUCED MODEL

Experimental Set-up

The experimental set-up (shown in Fig. 1) was built based on the test rig of EN 779:2012 –Particulate air filters for general ventilation-Determination of the filtration performance. The air flow rate is controlled by a variable frequency device (VFD), and measured by a nozzle flow meter. Polydisperse Aerosol DEHS (DiEthylHexylSebacate) is generated by a Laskin nozzle, which produces droplets in sufficient concentration in the size range of 0.2 µm to 3.0 µm. The DEHS is used to calculate the efficiency of the test filter. In the mixing chamber, the aerosol for efficiency testing is dispersed and mixed to create a uniform concentration. Loading dust is ASHRAE dust (composed, by weight, of 72% ISO A2 dust (fine), 23% powdered carbon and 5% milled cotton linters), fed by the dust feeder. Outdoor air particles are filtrated by coarse filter and HEPA filter, preventing outdoor particles affecting the experimental results. Meanwhile, a final filter classified as F9 according to EN 779:2012 standard collects particles passing through the test filter to calculate dust holding mass and also avoid causing indoor air pollution. An optical particle counter (OPC) was used to sample air and record particle concentration upstream and downstream of the tested filter.

10 clean filters were purchased from different manufacturers for use in the experiment to validate the deduced penetration model during dynamic filtration and obtain the coefficient. The detailed information of the tested filters was shown in Table 1. There were 7 V-bank filter samples made of glass fiber with different efficiencies, and 3 bag filter samples made of non-woven fabric with different efficiencies. The flow rate for all filter samples is 3400 m^3/h and Classification of filters is based on EN 779:2012.

Experimental Procedures

The validation experiments were carried out according to the procedures specified in the EN779 Standard. Tested filter sample and final filter were weighed first, and then sealed into a duct in a manner that prevents leakage. The fan was turned on to check if the tunnel was sealed well and value of initial pressure drop was recorded at test flow rate.

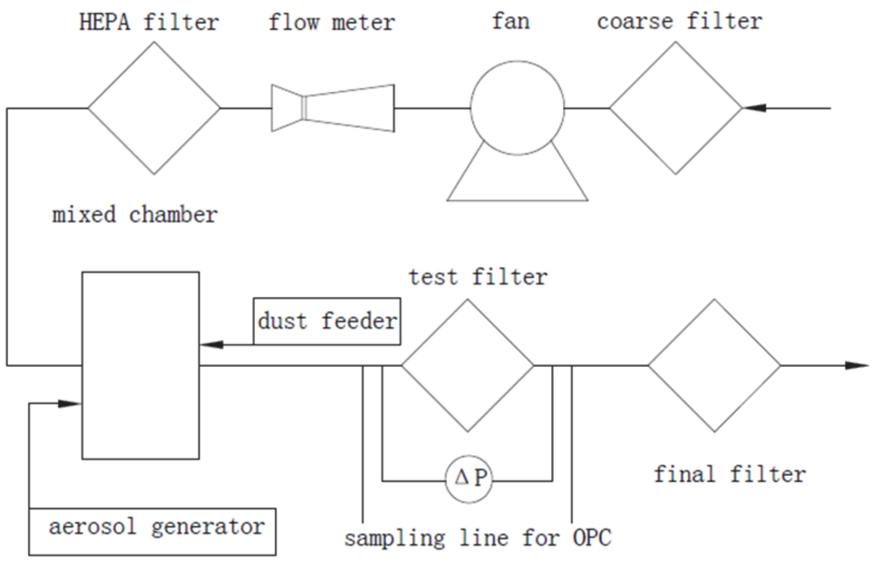

Fig. 1. Experimental set-up.

Table 1. Test filters.

Test filter	Sample	Dimension (mm)	Filter material	Classification
V-bank filter	1#	592 × 592 × 292	Glass fiber	F7
V-bank filter	2#	592 × 592 × 292	Glass fiber	M6
V-bank filter	3#	592 × 592 × 292	Glass fiber	M6
V-bank filter	4#	592 × 592 × 292	Glass fiber	F7
V-bank filter	5#	592 × 592 × 292	Glass fiber	F7
V-bank filter	6#	592 × 592 × 292	Glass fiber	F9
V-bank filter	7#	592 × 592 × 292	Glass fiber	F8
Bag filter	8#	592 × 592 × 550-8P	Non-woven fabrics	M6
Bag filter	9#	592 × 592 × 550-8P	Non-woven fabrics	F8
Bag filter	10#	592 × 592 × 550-8P	Non-woven fabrics	F7

The aerosol generator output was adjusted to generate a stable concentration of aerosol within the OPC coincidence level requirements and such that the downstream count rate was sufficient for a statistically valid result within an acceptable time scale. The efficiency measurement was done by a series of 13 counts of a minimum 20 seconds conducted successively upstream and downstream of the filter under test and with a purge before each count, or with one intervening sample upstream or downstream without counting, in order to stabilize the concentration of particles in the transfer lines. The efficiency E at 0.4 µm, 0.6 µm, 0.8 µm, 1.4 µm was calculated as follows:

$$E = \left[1 - \frac{n_i}{N_i}\right] \times 100\% \tag{29}$$

where n_i and N_i are the average number of particles in the size range "i" downstream of filter and upstream of filter, respectively.

The dust loading procedure was performed after the above procedure was finished for clean filter. When the filter was progressively filled with test dust, pressure drop and efficiency consequently changed. At the first dust loading stage, 30 g dust increments were fed at a concentration of 70 mg/m^3. The filter was air-swept for five minutes to reduce emission of particles "released" from the partly loaded filter and from inside duct system. The releasing, re-entrainment or shedding of particles after five minutes was included in the measurement and would influence the efficiency determination. Pressure drop and weight of final filter were recorded while the efficiency was measured in the same way as for initial efficiency.

According to the test, final recommendation pressure drop (450 Pa) and pressure drop of the first dust loading stage, the following dust loading procedure was divided into 4 stages. At these stages, dust increments were weighed to ± 0.1 g, and dust was also fed to the filter at a concentration of 70 mg/m^3 until each pressure drop step value was attained. Before stopping the dust feeding, whatever dust remained in the feeder tray was brushed to the dust pickup tube so that it was entrained in the duct air flow. Air-sweep for five minutes was also done. Pressure drop, efficiency of test filter, fed dust, and final filter weight were measured at each stage.

Since filter pressure drop continued rising during the whole test period, the fan frequency was controlled in order to remain the test air flow rate unchanged during the whole period of dust loading. At the end of test, test dust deposited upstream of test filter was collected for correcting the fed dust weight.

A procedure was used to determine whether the filter efficiency was dependent on the electrostatic removal mechanism. This was accomplished by measuring the removal efficiency of an untreated filter material and the corresponding efficiency after the effect of the electrostatic removal mechanism had been eliminated or inhibited. Isopropanol (IPA) was used to discharge filter material and the detailed procedure was based on the requirements specified in EN 779:2012.

RESULTS AND DISCUSSION

Determination of Efficiency Change with Dust-loaded Mass

To determine whether the filter test efficiency was dependent on the electrostatic removal mechanism, the removal efficiency of an untreated filter material and the corresponding efficiency after the effect of the electrostatic removal mechanism had been eliminated by isopropanol were measured. Results showed that the efficiency at 0.4 µm discrepancies between untreated and treated media do not exceed 0.5% for all sample material, therefore, the effect of the electrostatic removal mechanism could be ignored in this experiment. The results of the experiments for determining changes in filtration efficiency of different particle diameters as a function of the dust-loaded mass in test filters are shown in Figs. 2(a)–2(d). 10 samples show a similar trend between dust-loaded mass and efficiency, therefore, only sample 1#, 3#, 6#, 10# test filters are taken for examples. Sample 1#, 3# and 6# are V-bank filters with different average efficiencies, and sample 10# filter is bag filter.

It could be seen from the figures that filtration efficiency of different diameter increases rapidly with dust holding mass at the early stage of clogging, then, the rate of increase becomes slower along with the amount increase of dust. This may be caused by change of filtration from depth to surface filtration. The rates of efficiency growth for different particle diameter are different, among which, largest at 0.4 µm and smallest at 1.4 µm, respectively. The cause of this phenomenon is that the initial efficiency of large particles is high; hence, effect of deposited dust on the efficiency is relatively small. Sample 6# filter has high initial efficiencies at 0.8 µm and 1.4 µm with 99.9% and 100% respectively, therefore, the efficiencies are almost constant.

Validation of Dynamic Penetration Model

Figs. 3(a)–(d) reveal the relationship between experimental penetration of clogging filter and dust-loaded mass. It can be found that there is a linear relationship between $-\ln P_M$ and M, which verifies the correction of penetration model-Eq. (28). It also could be known that growth rate varies for different filter and particle diameter. The other tested samples (2#, 4#, 5#, 7#, 8#, 9#) have similar results.

The coefficient K for four different aerosol particle diameters is presented in Fig. 4. It appears that value of K decreases along with increase of the aerosol particle diameter for a filter. Moreover, the growth rate of efficiency decreases when aerosol particle diameter increases for a filter. It is obvious that the value of K stands for the efficiency growth rate. The larger value of coefficient K, the higher rate of efficiency growth. The values of K for sample 6# filter at 0.8 µm and 1.4 µm aerosol particles are zero, which was due to the fact that penetrations are constant during clogging.

According to EN 779, average efficiencies at 0.4 µm for ten sample filters were calculated. The average efficiency is an efficiency averaged to take account of the effects of progressive dust loading. For a series of "n" dust loading phases, the average efficiency is given by the following formula:

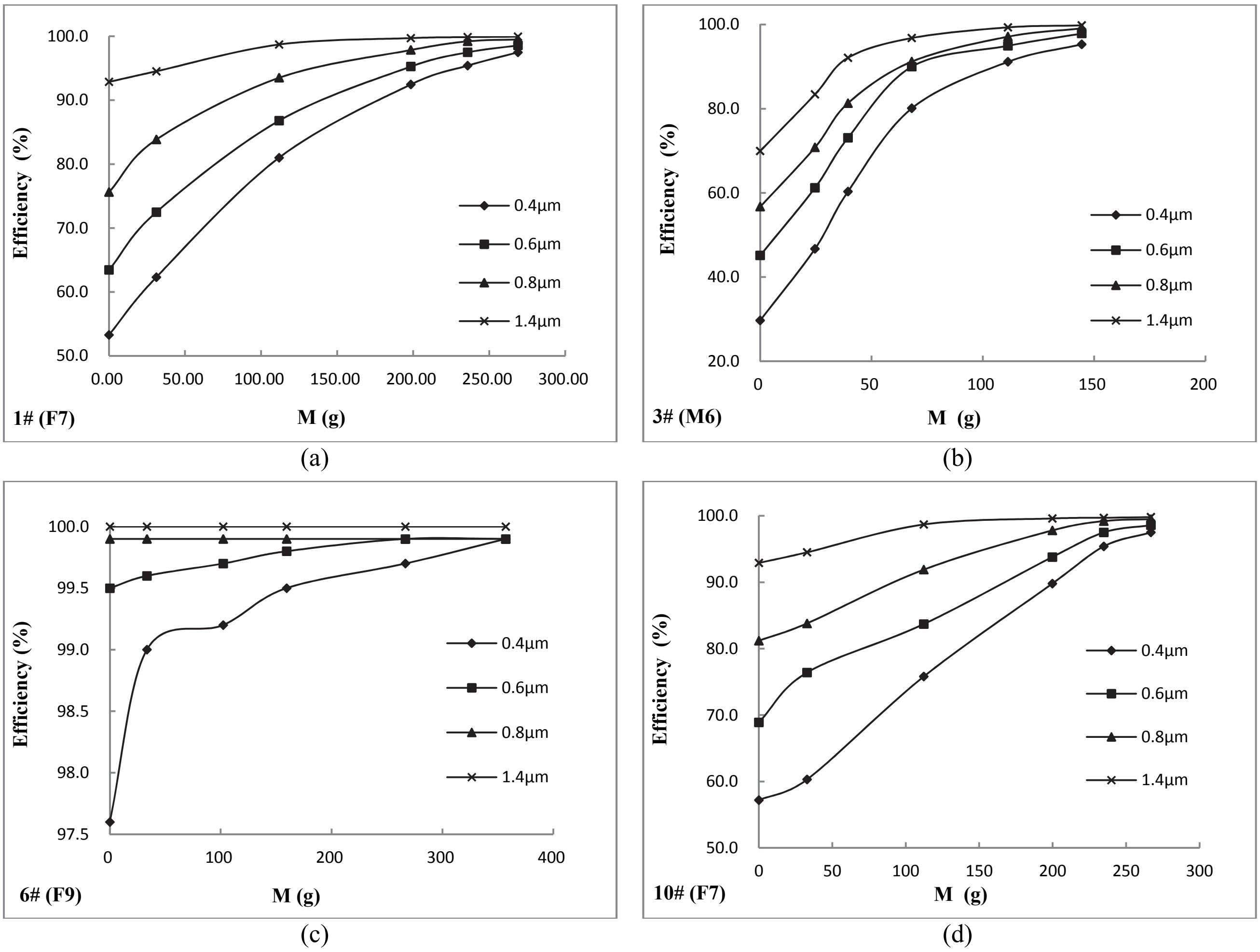

Fig. 2. Efficiency as a function of dust holding mass for 0.4 µm, 0.6 µm, 0.8 µm, 1.4 µm aerosol particles.

$$E_m = \frac{1}{M}\sum_{j=1}^{n}\left(\frac{E_{(j-1)}+E_j}{2}\times M_j\right) \quad (30)$$

where E_m is the average efficiency for all dust loading stages, E_j is the average efficiency after the dust loading phase "j", $M = \sum_{j=1}^{n} M_j$.

Figs. 5(a)–5(d) are the results for V-bank sample filters. It can be seen that K value change with average efficiencies for all aerosol particle diameters. Along with average efficiency increasing, decline of coefficient K becomes slower, which indicates K is related to filter efficiency for a given aerosol particle size. The relationship between coefficient K and average efficiency for different aerosol particle diameter can be expressed as:

$$\mathrm{K} = \varepsilon e^{\theta E_m} \quad (31)$$

Therefore, coefficient K for different particle diameter could be obtained when average efficiency is known.

Coefficients for bag filters have the same characteristics as those for V-bank filters shown in Fig. 5, i.e., K value decreases with filter average efficiency increasing. However, this trend does not exist for different material filters. Fig. 6 shows the comparison of K for the filters with different types of filter material. It can be seen from the figure that a filter (point a in Fig. 6) made of no-woven fabric with higher efficiency, however, with larger value of K, compared with the filter (point b in Fig. 6) made of glass fiber. This suggests that in addition to average efficiency and aerosol particle size, the filter material media may also affect the value of coefficient K.

All results presented are for ASHRAE dust and only applicable for the tested cases. Future research would therefore not only take into account testing different filters, but also different loading dusts, including filters aged in real applications to check for the applicability of the model.

CONCLUSIONS

This study developed a model to quantitatively describe penetration change during dust loading in a fiber filter, which indicates that filter penetration is a function of coefficient K and mass deposited in the filter. This model is deduced from two different methods. One is ignoring the specific deposit structure, and assuming captured particles

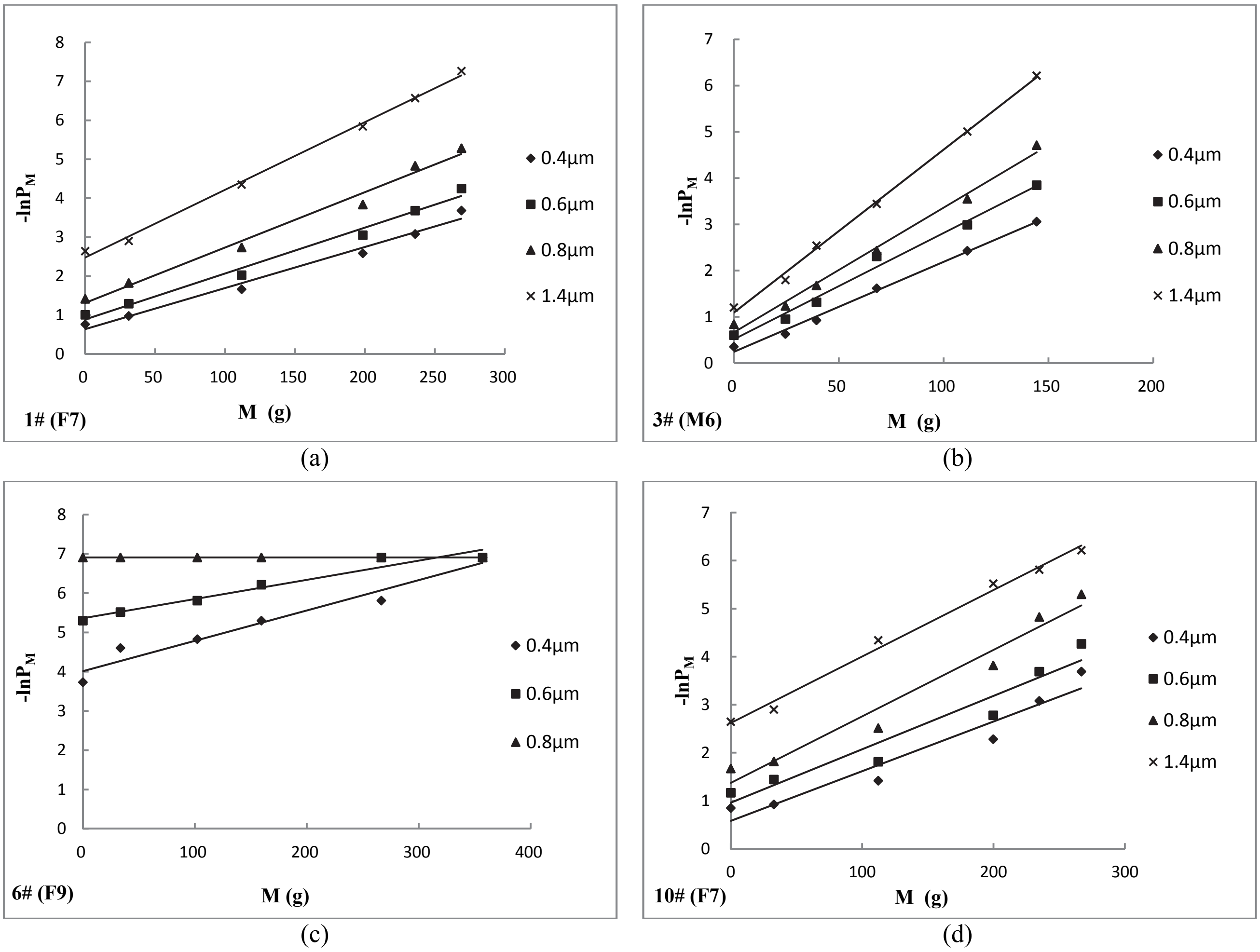

Fig. 3. $-\ln P_M$ as a function of dust holding mass for 0.4 μm, 0.6 μm, 0.8 μm, 1.4 μm aerosol particle.

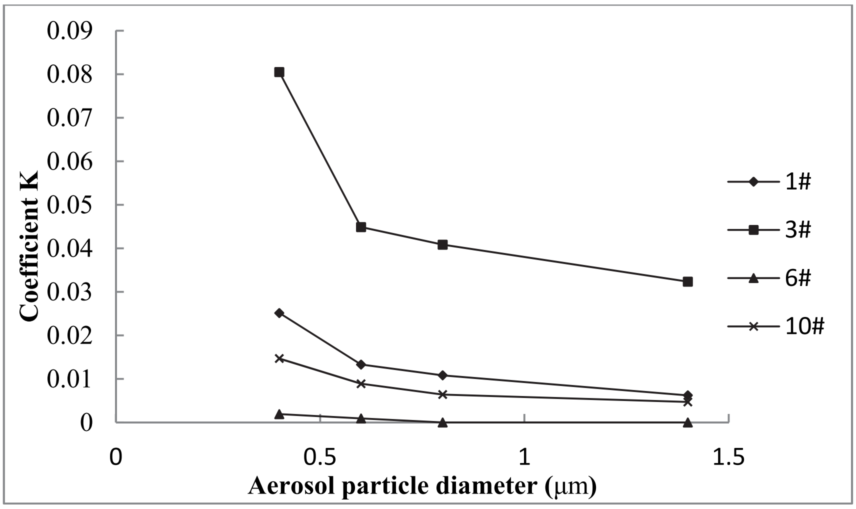

Fig. 4. Coefficient K vs. aerosol particle diameter for sample 1#(F7), 3#(M6), 6#(F9), 10#(F7) test filters.

fill the filter, the fiber filter material becomes more compact. The other is assuming the whole fibrous filter material as a single long fiber, and applying collection efficiency of a particle-loaded single fiber. The two formulas of penetration using different methods are in accordance with each other.

The experiments with 10 sample filters were carried out to validate the developed model, and the coefficient K is obtained using regression analysis through the results of experiments. A large value of K appears to illustrate the rapid rate increase in efficiency. Aerosol particle diameter,

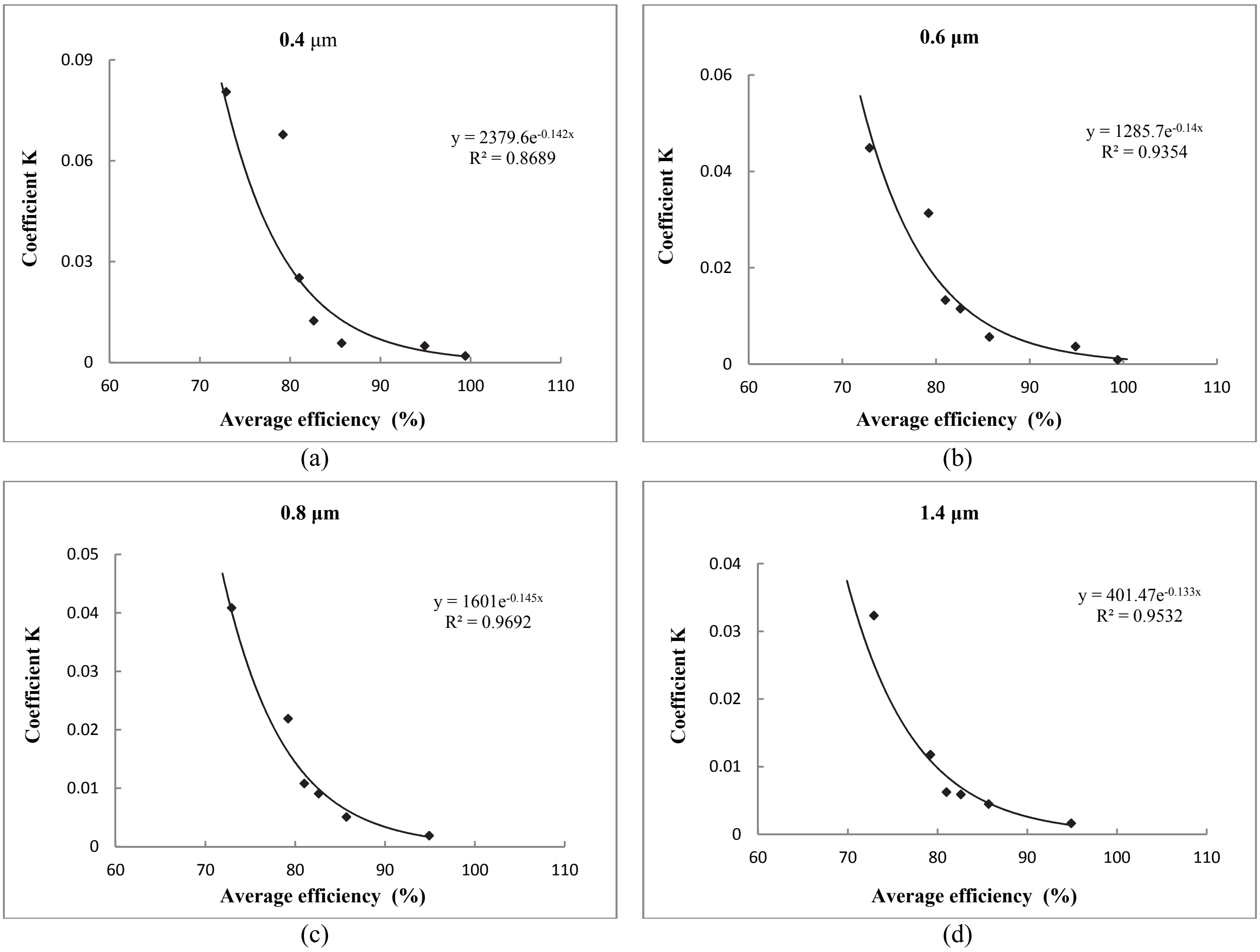

Fig. 5. Coefficient K as a function of average efficiency for 0.4 µm (a), 0.6 µm (b), 0.8 µm (c),1.4 µm (d) aerosol particle.

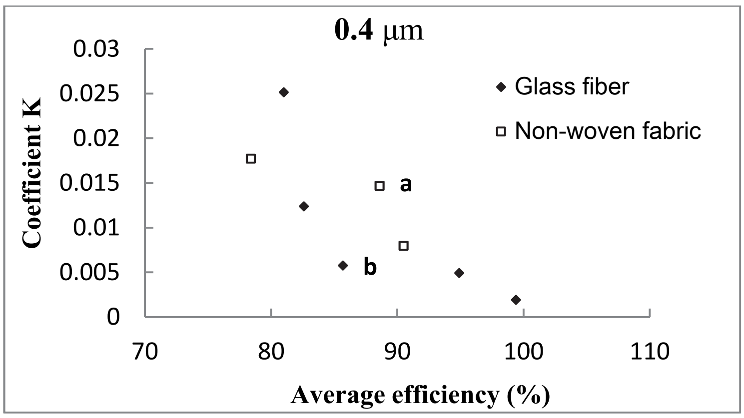

Fig. 6. Comparison of coefficient K for non-woven fabrics and glass fiber at 0.4 µm aerosol particle.

efficiency and material of filter affect the value of K. The value of K for smaller aerosol particle and higher penetration filter are bigger.

More filters need to be tested in future work in order to collect sufficient experimental data to ensure the value of K for different aerosol particles and different efficiency filters. With a known value of coefficient K, penetration change could be predicted in actual applications using the developed model. On the other hand, the relationship between penetration and pressure drop during filter clogging might also be established based on this model and those for pressure drop change with dust mass collected in a filter.

ACKNOWLEDGE

This work was supported by NIPPON MUKI CO., LTD.

REFERENCES

Barot, D.T., Tien, C. and Wang, C.S. (1980). Accumulation of Solid Particles on Single Fibers Exposed to Aerosol Flows. *AlChE J.* 26: 289–292.

Bhutra, S. and Payatakes, A.C. (1979). Experimental Investigation of Dendritic Deposition of Aerosol Particles. *J. Aerosol Sci.* 10: 445–464.

Billings, C.E. (1966). Effects of Particle Accumulation in Aerosol Filtration. Ph.D. Dissertation, California Institute of Technology, Pasadena, USA.

Davies, C.N. (1970). The Clogging of Fibrous Aerosol Filters. *J. Aerosol Sci.* 1: 35–39.

Dunnett, S.J. and Clement, C.F. (2006). A Numerical Study of the Effects of Loading from Diffusive Deposition on the Efficiency of Fibrous Filters. *J. Aerosol Sci.* 37: 1116–1139.

Endo, Y., Chen, D.R. and Pui, D.Y.H. (1998). Effects of Particle Polydispersity and Shape Factor during Dust Cake Loading on Air Filters. *Powder Technol.* 98: 241–249.

Hinds, W.C. (1999). *Aerosol Technology: Properties, Behavior, and Measurement of Airborne Particle*, John Willey & Sons, Inc., New York.

Hosseini, S.A. and Vahedi Tafreshi, H. (2012). Modeling Particle-loaded Single fiber Efficiency and Fiber Drag Using ANSYS–Fluent CFD Code. Computers & Fluids.

Kanaoka, C., Emi, H. and Myojo, T. (1980). Simulation of the Growing Process of a Particle Dendrite and Evaluation of a Single Fiber Collection Efficiency with Dust Load. *J. Aerosol Sci.* 11: 377–389.

Kanaoka, C., Emi, H., Myojo, T. and Mikio, O. (1980). Estimation of Collection Efficiency of Air Filter with Dust Load. *Chem. E. Symposium Series* 3: 1–15.

Kasper, G., Schollmeier, S., Meyer, J. and Hoferer, J. (2009). The Collection Efficiency of a Particle-loaded Single Filter Fiber. *J. Aerosol Sci.* 40: 993–1009.

Payatakes, A.C. and Tien, C. (1976). Particle Deposition in Fibrous Media with Dendrite-like Pattern: A Preliminary Model. *J. Aerosol Sci.* 7: 85–100.

Payatakes, A.C. (1977). Model of Transient Aerosol Particle Deposition in Fibrous Media with Dendritic Pattern. *AIChE J.* 23: 192–202.

Payatakes, A.C. and Gradoń, L. (1980a). Dendritic Deposition of Aerosol Particles in Fibrous Media by Inertial Impaction and Interception. *Chem. Eng. Sci.* 35: 1083–1096.

Payatakes, A.C. and Gradoń, L. (1980b). Dendritic Deposition of Aerosols by Convective Brownian Diffusion for Small, Intermediate and High Particle Knudsen Numbers. *AIChE J.* 26: 443–454.

Schmidt, E. and Löffler, F. (1990). Preparation of Dust Cakes for Microscopic Examination. *Powder Technol.* 60: 173–177.

Schmidt, E. and Löffler, F. (1991). The Analysis of Dust Cake Structures. *Part. Part. Syst. Char.* 8: 105–109.

Schmidt, E. (1995). Experimental Investigations into the Compression of Dust Cakes Deposited on Filter Media. *Filtr. Sep.* 32: 789–793.

Schmidt, E. (1997). Theoretical Investigations into the Compression of dust Cakes Deposited on Filter Media. *Filtr. Sep.* 34: 365–368.

Silva, C.R.N., Negrini, V.S., Aguiar, M.L. and Coury, J.R. (1999). Influence of Gas Velocity on Cake Formation and Detachment. *Powder Technol.* 101: 165–172.

Thomas, D., Penicot, P., Contal, P., Leclerc, D. and Vendel, J. (2001). Clogging of Fibrous Filters by Solid Aerosol Particles. Experimental and Modeling Study. *Chem. Eng. Sci.* 56: 3549–3561.

Wang, H., Zhao, H., Guo, Z. and Zheng, C. (2012). Numerical Simulation of Particle Capture Process of Fibrous Filters Using Lattice Boltzmann Two-phase Flow Model. *Powder Technol.* 227: 111–122.

Watson, J.H.L. (1946). Filmless Sample Mounting for the Electron Microscope. *J. Appl. Phys.* 17: 121–127.

Wright, T.E., Stasny, R.J. and Lapple, C.E. (1957). High Velocity Air Filters (No. AD-142075; WADC-TR-55-457). Donaldson Co., Inc., St. Paul.

Received for review, April 22, 2014
Revised, September 21, 2014
Accepted, September 23, 2014